

Sustainable and Resilient Infrastructure



ISSN: 2378-9689 (Print) 2378-9697 (Online) Journal homepage: http://www.tandfonline.com/loi/tsri20

Resilience analysis: a mathematical formulation to model resilience of engineering systems

Neetesh Sharma, Armin Tabandeh & Paolo Gardoni

To cite this article: Neetesh Sharma, Armin Tabandeh & Paolo Gardoni (2018) Resilience analysis: a mathematical formulation to model resilience of engineering systems, Sustainable and Resilient Infrastructure, 3:2, 49-67, DOI: 10.1080/23789689.2017.1345257

To link to this article: https://doi.org/10.1080/23789689.2017.1345257

	Published online: 24 Oct 2017.
	Submit your article to this journal 🗹
ılıl	Article views: 841
CrossMark	View Crossmark data 🗗
4	Citing articles: 1 View citing articles 🗹





Resilience analysis: a mathematical formulation to model resilience of engineering systems

Neetesh Sharma, Armin Tabandeh and Paolo Gardoni

Department of Civil and Environmental Engineering, MAE Center: Creating a Multi-hazard Approach to Engineering, University of Illinois at Urbana-Champaign, Urbana, IL, USA

ABSTRACT

The resilience of a system is related to its ability to withstand stressors, adapt, and rapidly recover from disruptions. Two significant challenges of resilience analysis are to (1) quantify the resilience associated with a given recovery curve; and (2) develop a rigorous mathematical model of the recovery process. To quantify resilience, a mathematical approach is proposed that systematically describes the recovery curve in terms of partial descriptors, called resilience metrics. The proposed resilience metrics have simple and clear interpretations, and their definitions are general so that they can characterize the resilience associated with any recovery curve. This paper also introduces a reliability-based definition of damage levels which is well-suited for probabilistic resilience analysis. For the recovery modeling, a stochastic formulation is proposed that models the impact of recovery activities and potential disrupting shocks, which could happen during the recovery, on the system state. For illustration, the proposed formulation is used for the resilience analysis of a reinforced concrete (RC) bridge repaired with fiber-reinforced polymer.

ARTICLE HISTORY

Received 8 February 2017 Accepted 5 June 2017

KEYWORDS

Life-cycle analysis; recovery; reliability: resilience: stochastic

1. Introduction

The prosperity of modern societies relies on the ability of infrastructure systems to deliver services and resources to human communities (Corotis, 2009; Ellingwood et al., 2016; Gardoni, Murphy, & Rowell, 2016). The safety assessment of such systems has been subject of much research (see, for example, Gardoni & LaFave, 2016). The resilience of infrastructure systems is another crucial attribute that has gained much attention within the engineering discipline over the past 10–15 years (Bruneau et al., 2003; Ellingwood et al., 2016; Guidotti, Gardoni, & Chen, 2017; Guidotti et al., 2016; McAllister, 2013). The resilience of a system integrates the system state in the immediate aftermath of a disruption, which is typically related to the system safety, with the recovery process to achieve a desirable system state (Mieler, Stojadinovic, Budnitz, Comerio, & Mahin, 2015). The challenges at the core of resilience analysis are to (1) quantify the resilience associated with a given system state and a selected recovery strategy (which together shape its recovery curve); and (2) develop a rigorous mathematical model of the recovery process.

We can determine the system state at any time in terms of quantities such as the instantaneous reliability or system functionality. A recovery curve represents the path of such quantities over the recovery duration. The recovery curve of a system is typically a non-decreasing function of time that can be continuous, discrete, or piecewise continuous. However, the occurrence of disrupting shocks at discrete points in time during the recovery can cause sudden drops in the recovery curve. Besides the potential disrupting shocks, there are other influencing factors such as the availability of resources for repair and weather conditions, which can affect the actual recovery.

Once properly defined, the recovery curve of a system provides the complete information about its resilience. Thus, to accurately quantify the resilience of the system, resilience metric(s) must capture all the relevant characteristics of the recovery curve. Mathematically, it follows that a single metric cannot generally replace a curve and capture all of its characteristics.

A number of studies have attempted to quantify the resilience of physical and organizational systems. Among the first contributions, Bruneau et al. (2003) quantified the resilience of a system as the integral of the recovery curve over time. Chang and Shinozuka (2004) quantified resilience in terms of the probability that a system's performance loss, right after a disruption, and the corresponding recovery time would be less than some thresholds. Several variants of the initial resilience metrics can be found in more recent studies, as in Decò, Bocchini, and Frangopol (2013) and Ayyub (2014). The significance of these initial contributions is to quantify the resilience of a system with a simple metric. However, as mentioned earlier, a single metric can only provide partial information about actual resilience. Furthermore, one cannot expand the existing resilience metrics in a systematic way, to provide the full description of the resilience of a system. As a result, the existing metrics do not fully characterize the recovery curves with different shapes and might not be able to distinguish among the different resilience levels.

For modeling the recovery process, Cimellaro, Reinhorn, and Bruneau (2010a) and Decò et al. (2013) proposed parametric functions for the recovery curves, the shapes of which are selected based on qualitative explanations of the recovery situation, such as the severity of the initial damage and preparedness of a system/society in responding to a disruptive event. To account for the uncertainty in the recovery modeling, probability distributions are assigned to the parameters of the functions. The analytical modeling of the recovery process facilitates the calculation of resilience, while incorporating the uncertainty. However, there remain questions regarding the accuracy of the parametric functions in replicating the actual situation of the recovery. In particular, due to the lack of explicit relation between the shape of the recovery curve and its influencing factors, it is not clear how new information such as ongoing progress of the work or increased resource availability may reduce the uncertainty involved in the recovery modeling (e.g. uncertainty in the choice of the parametric function for the recovery curve and statistical uncertainty in the estimate of the unknown model parameters). Furthermore, because the recovery modeling is at the system level, it is not generally possible to use the information (e.g. time and expenditure) gained from the recovery of one system to model the recovery of another system. Finally, these approaches cannot take advantage of the information available at the level of individual recovery activities (which collectively determine the scope of work at the system level).

This paper proposes a rigorous mathematical formulation for resilience analysis. In this formulation, we characterize the resilience associated with a given system state, in the immediate aftermath of a disruption, and for a selected recovery strategy by proposing resilience metrics, which form a complete set of partial descriptors of the recovery curve. Such metrics have two desirable properties: (1) they are simple and have clear interpretations, and (2)

it is possible to expand a given (sub-)set of metrics with additional ones in a systematic way to provide further information about system resilience up to capturing the entire information in the recovery curve. The first property facilitates the understanding and communication of the level of resilience of a system to the public and increases the public involvement in the decision-making process. The second property enables the formulation to characterize the resilience associated with any given system state and a selected recovery strategy with the desired level of accuracy.

Developing the recovery strategy and modeling the recovery process begins with determining the damage level. We propose a reliability-based definition of damage levels, which accounts for safety considerations and is ideally suited for the probabilistic resilience analysis. For the recovery modeling, we develop a stochastic formulation that models the impact of recovery activities and disrupting shocks (which could happen during the recovery) on the system state. The key elements of the proposed formulation are: (1) modeling the completion time of the recovery steps (a group of recovery activities that improve the reliability of the system), and the occurrence time of disrupting shocks, and (2) predicting the system state after the completion of each recovery step or the occurrence of a disrupting shock. We model the completion times of the recovery steps as a general Poisson process with a mean function that accounts for the recovery condition (e.g. required recovery activities, the availability of resources, weather condition). The occurrence times of disrupting shocks generally depend on the type of hazard considered in the formulation. The proposed formulation can employ hazard specific predictive models for this purpose (e.g. a Poisson or Renewal process to model the occurrence of seismic shocks). When planning the recovery, the desired values of variables that define a system, also called state variables, such as material properties, are specified after the completion of each recovery step. We use such state variables in existing capacity and demand models to determine the corresponding system state after each recovery step. To model the impact of disrupting shocks, we use the models proposed by Jia and Gardoni (2017a) to determine the impact on the state variables. As in the case of the recovery steps, we use the predicted values of the state variables in existing capacity and demand models to determine the system state. We illustrate the proposed formulation, considering the resilience analysis of a reinforced concrete (RC) bridge, repaired with Fiber Reinforced Polymer (FRP) composites.

The rest of the paper is organized into seven sections. The next section presents the proposed mathematical formulation of resilience analysis and the proposed resilience metrics. Section 3 illustrates the phases of the recovery

process and their role in resilience quantification. Section 4 describes the definition and role of instantaneous reliability, and its relation with system functionality. Section 5 explains the proposed stochastic formulation to model the recovery process. Section 6 discusses the solutions of quantities of interest. Section 7 presents a numerical example to illustrate the proposed formulations. Finally, we summarize the contributions and draw some conclusions.

2. Proposed resilience metrics and mathematical formulation for resilience analysis

Assessing the resilience of engineering systems is crucial both for pre-disruption effective mitigation planning and post-disruption optimal resource allocation. There are many factors that influence the resilience of engineering systems, including the design specifications, the availability of resources needed for the repairs (e.g. funding and materials), the accessibility of damaged components, preparedness of recovery plans, and environmental condition during the recovery.

In this section, we first review the current practice of resilience quantification, the available metrics and their limitations. Then, we propose a new mathematical formulation for resilience analysis based on which we develop new resilience metrics that overcome the current limitations.

Figure 1 shows a typical recovery curve used in the literature to quantify resilience (Bocchini, Decò, & Frangopol, 2012; Bonstrom & Corotis, 2016; Cimellaro, Reinhorn, & Bruneau, 2010b). An external shock (e.g. an earthquake) at time t_I causes an instantaneous reduction in the system state, represented by an indicator, Q(t), (e.g. the system functionality). The residual system state, $Q_{\rm res}$, depends on the intensity of the shock, design specifications, and the system state before the shock.

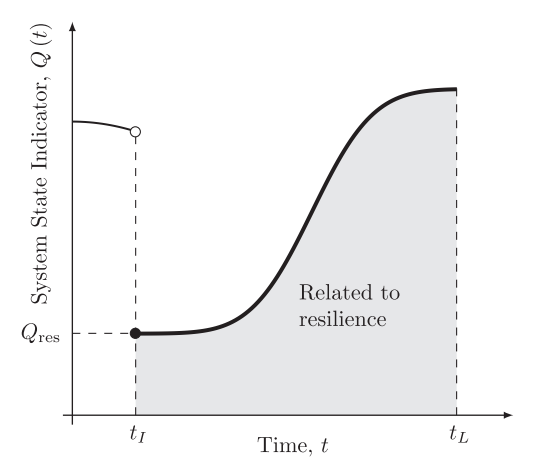


Figure 1. A typical recovery curve used in the literature to quantify resilience.

Subsequently, the system undergoes a recovery process to achieve a desired Q(t) (e.g. the original functionality or a higher one, if desired). After meeting the desired requirements, the recovery process terminates at time t_L . The impact of resilience influencing factors, listed earlier, would be reflected in the shape of the recovery curve and the recovery time, $T_R := t_L - t_T$. The resilience of the system is typically quantified as a function of the shaded area in Figure 1.

Mathematically, the typical resilience metric (see, for example, Bonstrom & Corotis, 2016; Bruneau & Reinhorn, 2007; Cimellaro et al., 2010b) is defined as

$$R: = \frac{\int_{t_{l}}^{t_{L}} Q(t)dt}{T_{R}} = \frac{\int_{0}^{T_{R}} \breve{Q}(\tau)d\tau}{T_{R}},$$
 (1)

where we use the change of variable $\tau = t - t_I$ and define $\check{Q}(\tau)$: = Q(t). The limitation of the resilience metric, R, is that it gives the same value of resilience for different combinations of $\check{Q}(\tau)$ and T_R . We explain this limitation with the following example. Consider the three possible recovery curves in Figure 2. Table 1 summarizes the mathematical expressions for the three recovery curves and their T_R 's. The three different recovery curves correspond to different levels of resilience (e.g. the curve *Linear 1* might be considered the most desirable recovery). However, as shown in Table 1, the values of R for the three recovery curves are the same (i.e. all equal to 0.75).

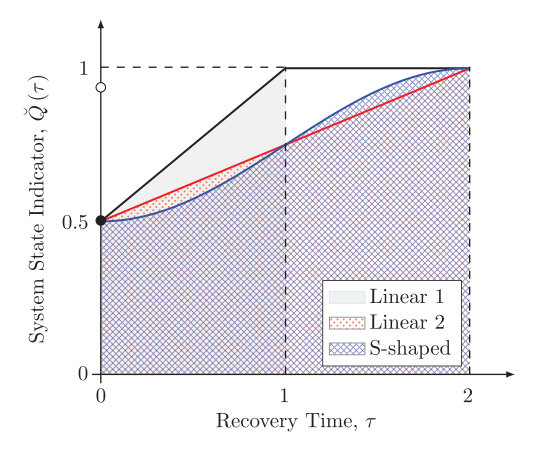


Figure 2. The current resilience metrics cannot differentiate the resilience associated with the three different recovery curves.

Table 1. The mathematical expressions of the recovery curves in Figure 2 and the associated resilience metric *R*.

Description	T_R	Recovery function	R	$R(t_H = 2)$	$R(t_H = 3)$
Linear 1	1	0.5 + 0.5 t	0.75	0.87	0.92
Linear 2	2	0.5 + 0.25 t	0.75	0.75	0.83
S-shaped	2	$0.75 - 0.25 \cos(\pi t/2)$	0.75	0.75	0.83

To distinguish the resilience associated with the recovery curves having different T_p 's (e.g. recovery curves *Linear* 1 and Linear 2 in Figure 2), Reed, Kapur, and Christie (2009) proposed a different definition of R by replacing t_{τ} in Equation (1) with a fixed time horizon t_{τ} (the same formulation was also used in Cimellaro et al., 2010a; Decò et al., 2013). Let us denote the metric in Reed et al. (2009) as $R(t_H)$. The value of $R(t_H)$ for a given system and a fixed t_{I} can change with t_{II} though the ability of the system to recover (i.e. its resilience) may remain unchanged. The last two columns of Table 1 summarize the values of $R(t_{ij})$ associated with the three recovery curves in Figure 2, considering $t_H = 2$ and $t_H = 3$ (both with $t_I = 0$). The values of $R(t_{\mu})$ for each of the three recovery curves increase as t_{μ} increases; however, the ability of the system to recover (i.e. the recovery curve) remains unchanged. Furthermore, $R(t_H)$, for the selected values of t_H , does not distinguish the resilience associated with the recovery curves having different trends (i.e. recovery curves *Linear 2* and *S-shaped*).

We propose a new resilience analysis that quantifies the resilience associated with a given recovery curve in terms of the partial descriptors of $\dot{Q}(\tau)$. The proposed partial descriptors are inspired by those in probability theory and mechanics. The analogy between the proposed resilience metrics and those in probability theory and mechanics is described later in this section after the proposed resilience metrics are defined. To explain the proposed resilience analysis, we first develop the tools for describing the recovery process and then derive the partial descriptors. The recovery curve $Q(\tau)$ that we term the Cumulative Resilience Function (CRF), hereafter, represents the overall recovery progress by time τ . Once $\tilde{Q}(\tau)$ is specified, we can obtain the Instantaneous Rate of the Recovery Progress according to the following three mathematical formulations.

Definition 1: When the CRF is a continuous function of time, the instantaneous rate of recovery progress is the time derivative of the CRF. Mathematically, we can write it as $q(\tau) = d\dot{Q}/d\tau$ for all $\tau \in [0, T_R]$, which we call the Resilience Density Function (RDF). The RDF is undefined at a possible finite set of points where the derivative of the CRF does not exist (i.e. CRF is a continuous function of class C^0). We can obtain the recovery progress over any time interval $(\tau_u, \tau_v] \subseteq [0, T_R]$ as follows:

$$\check{Q}\left(\tau_{u} < \tau \leq \tau_{v}\right) = \int_{\tau}^{\tau_{v}} q(\tau)d\tau.$$
(2)

Definition 2: When the CRF is a step function, we can no longer define the RDF because of the discontinuity in the CRF. In such cases, we define the Resilience Mass Function (RMF) as $q(\tau) = \sum_{k=0}^{\infty} \Delta \breve{Q}(\tau_k) \delta(\tau - \tau_k)$, for all $\tau \in [0, T_R]$ where $\Delta \mathring{Q}(\tau_k) := \mathring{Q}(\tau_k) - \mathring{Q}(\tau_k^-)$ is the size of the jump in CRF at the discontinuity point $\tau = \tau_k$ (where τ_0 : = 0); τ_k^- is the time instant immediately before τ_k ; and $\delta(\cdot)$ is the Dirac delta function. Similar to the continuous case, we can obtain the recovery progress over any time interval $(\tau_u, \tau_v] \subseteq [0, T_R]$ as

$$\check{Q}(\tau_{u} < \tau \leq \tau_{v}) = \int_{\tau_{u}}^{\tau_{v}} \sum_{k=0}^{\infty} \Delta \check{Q}(\tau_{k}) \delta(\tau - \tau_{k}) d\tau$$

$$= \sum_{k=0}^{\infty} \Delta \check{Q}(\tau_{k}) \mathbf{1}_{\{\tau_{u} < \tau_{k} \leq \tau_{v}\}}, \tag{3}$$

where $\mathbf{1}_{\{ au_u < au_k \le au_v\}}$ is an indicator function such that $\mathbf{1}_{\{ au_u < au_k \le au_v\}} = \mathbf{1}$, when $au_k \in (au_u, au_v]$ and $\mathbf{1}_{\{ au_u < au_k \le au_v\}} = 0$, otherwise. To reflect that at τ_0 the CRF is equal to Q_{res} (typically non-zero), we define $\Delta \tilde{Q}(0)$: = Q_{res} .

Definition 3: In general, the CRF might be a combination of the previous two cases (i.e. $\check{Q}(\tau)$ is a piecewise continuous function). In this case, we write the instantaneous rate of recovery progress as

$$q(\tau) = \tilde{q}(\tau) + \sum_{k=0}^{\infty} \Delta \tilde{Q}(\tau_k) \delta(\tau - \tau_k), \quad \tau \in [0, T_R] , \quad (4)$$

where $\tilde{q}(\tau)$ is the RDF, corresponding to the continuous part of the CRF, and $\Delta \hat{Q}(\tau_{\nu})\delta(\tau-\tau_{\nu})$ is the RMF, accounting for the discontinuities of the CRF. Accordingly, we can write the recovery progress over $(\tau_u, \tau_v] \subseteq [0, T_R]$ as

$$\check{Q}\left(\tau_{u} < \tau \leq \tau_{v}\right) = \int_{\tau_{u}}^{\tau_{v}} \tilde{q}(\tau)d\tau + \sum_{k=0}^{\infty} \Delta \tilde{Q}\left(\tau_{k}\right) \mathbf{1}_{\left\{\tau_{u} < \tau_{k} \leq \tau_{v}\right\}} \cdot (5)$$

The CRF or RDF/RMF of a system provides complete information about its residual state, the recovery process and, thus, its resilience. To help in the interpretation of the CRF, RDF, and RMF, one can see the analogy between their definitions and those of the Cumulative Distribution Function (CDF), Probability Density Function (PDF) and Probability Mass Function (PMF) that are used to describe random variables in probability theory.

To capture the degree of disparity between any pairs of recovery curves, we define the measure of Resilience Disparity, $\Delta(q_1, q_2)$, as follows:

$$\Delta(q_{1}, q_{2}) := \frac{\int_{0}^{T_{R}} q_{1}(\tau) \log_{2} \left[q_{1}(\tau) / \bar{q}(\tau) \right] d\tau + \int_{0}^{T_{R}} q_{2}(\tau) \log_{2} \left[q_{2}(\tau) / \bar{q}(\tau) \right] d\tau}{\check{Q}_{1}(T_{R_{1}}) + \check{Q}_{2}(T_{R_{2}})}, \quad (6)$$

where T_{R_1} and T_{R_2} are the recovery durations corresponding to q_1 and q_2 ; $T_R = \max(T_{R_1}, T_{R_2})$; and $\bar{q}(\tau) := [q_1(\tau) + q_2(\tau)]/2$. The resilience disparity is bounded between 0 and 1 such that $\Delta(q_1, q_2) = 0$, when $q_1(\tau) = q_2(\tau)$ for every $\tau \in [0, T_R]$ and $\Delta(q_1, q_2) = 1$, when $q_1(\tau) = 0$ corresponds to $q_2(\tau) > 0$ and, conversely, $q_2(\tau) = 0$ corresponds to $q_1(\tau) > 0$, for every $\tau \in [0, T_R]$. The proposed resilience disparity measure is analogous to divergence measures in probability theory. Specifically, when the CRFs are replaced with CDFs, $\Delta(q_1, q_2)$ corresponds to the Jensen-Shannon entropy (Lin, 1991).

Besides the resilience disparity, which gives a general comparison of $q(\tau)$'s, partial descriptors can be defined to capture specific characteristics of the resilience. First, we can define the central measures of resilience. We define the Center of Resilience, ρ_{O} , as

$$\rho_{Q} := \frac{\int_{0}^{T_{R}} \tau q(\tau) d\tau}{\int_{0}^{T_{R}} q(\tau) d\tau} = \frac{Q_{\text{res}}}{Q_{\text{tar}}} \rho_{Q,\text{res}} + \frac{\bar{Q}_{\text{res}}}{Q_{\text{tar}}} \rho_{\bar{Q},\text{res}}, \quad (7)$$

where $Q_{\rm res}/Q_{\rm tar}$ is the contribution of the residual state to ρ_Q , in which $Q_{\rm tar} := \check{Q}(T_R); \; \rho_{Q,\rm res} := \tau_0$ is the center of resilience, when considering only the residual state; \bar{Q}_{res}/Q_{tar} is the contribution of the recovery process to ρ_{Q} , in which $\bar{Q}_{\mathrm{res}} := Q_{\mathrm{tar}} - Q_{\mathrm{res}}$; and the $\rho_{\bar{Q},\mathrm{res}} := \left[\int_0^{T_R} \tau \tilde{q}(\tau) d\tau + \sum_{k=1}^{\infty} \tau_k \Delta \tilde{Q}(\tau_k) \mathbf{1}_{\{0 \le \tau_k \le T_R\}} \right] / \bar{Q}_{\mathrm{res}}$ is the center of resilience, when considering only the recovery process. Because $\tau_0 = 0$, Equation (7) simplifies into

$$\rho_{Q} = \frac{\bar{Q}_{res}}{Q_{tar}} \rho_{\bar{Q}, res}.$$
 (8)

The proposed expression for ρ_{O} distinguishes between the role of the residual system state (which affects \bar{Q}_{res}) the recovery process (which affects $\rho_{\bar{O}, \text{res}}$) in the quantification of resilience. Being able to decouple the two contributions facilitates the determination of the acceptable level of resilience in terms of a balance between the residual system state and the corresponding recovery duration. We also note that the value of ρ_O depends on the choice for $\tilde{Q}(\tau)$ (e.g. functionality or instantaneous reliability). Specifically, the different choices of $\check{Q}(\tau)$ affect the scale of variation, \bar{Q}_{res}/Q_{tar} , in Equation (8). As a result, the interpretation of the obtained results for ρ_O and decisions about the acceptable level of resilience depend on the choice of $Q(\tau)$.

Two other central measures are the Median of Resilience and the *Mode of Resilience*. The *Median of Resilience*, $\rho_{O.0.5}$, is the time instant at which the CRF is equal to $\tilde{Q}(T_p)/2$. The Mode of Resilience is the time instant corresponding to the maximum value of the instantaneous rate of recovery progress. Mathematically, we can write it as $\rho_{Q,\max} = \arg\max_{\tau \in [0,T_R]} q(\tau).$

We extend our definitions of the partial descriptors and introduce the measures of dispersion of the recovery process. We define the *Resilience Quantile*, $\rho_{O,w}$, which is the time instant corresponding to the *w*th $(0 \le w \le 1)$ quantile of the CRF. Mathematically, we write the resilience quantile as $\rho_{O,w} = \min\{\tau \in [0, T_R]: w \le [\mathring{Q}(\tau)/\mathring{Q}(T_R)]\}.$ The median of resilience, $\rho_{0.0.5}$, is a special case for which w = 0.5. Using $\rho_{O,w}$, we can define different measures of dispersion as the length of the intervals $[\rho_{Q,w_i}, \rho_{Q,w_i}]$, where $0 \le w_i < w_i \le 1$. We also define an alternative single measure to capture the dispersion that we call the Resilience *Bandwidth*, χ_0 , and mathematically, we write it as

$$\chi_{Q}^{2} := \frac{\int_{0}^{T_{R}} \left(\tau - \rho_{Q}\right)^{2} q(\tau) d\tau}{\int_{0}^{T_{R}} q(\tau) d\tau}$$

$$= \frac{1}{\breve{Q}\left(T_{R}\right)} \left[\int_{0}^{T_{R}} \left(\tau - \rho_{Q}\right)^{2} \widetilde{q}(\tau) d\tau + \sum_{k=0}^{\infty} \left(\tau_{k} - \rho_{Q}\right)^{2} \Delta \widetilde{Q}\left(\tau_{k}\right) \mathbf{1}_{\left\{0 \le \tau_{k} \le T_{R}\right\}} \right]. \tag{9}$$

The small values of χ_0 represent a situation in which a large percentage of the recovery process is completed over a short period of time around ρ_0 . In contrast, the large values of χ_0 describe a situation in which the recovery process is spread over a long period of time. We can also define the Relative Resilience Bandwidth as χ_0/T_R , which describes the spread of the recovery process with respect to the total recovery time, and the Bandwidth Coefficient as χ_0/ρ_0 , which describes the spread of the recovery process with respect to the center of resilience.

Another useful measure is the skewness of the recovery process. Mathematically, we can write the Resilience Skewness, ψ_0 , as

$$\begin{split} \psi_{Q} &:= \frac{\int_{0}^{T_{R}} \left(\tau - \rho_{Q}\right)^{3} q(\tau) d\tau}{\int_{0}^{T_{R}} q(\tau) d\tau} \\ &= \frac{1}{\breve{Q}\left(T_{R}\right)} \left[\int_{0}^{T_{R}} \left(\tau - \rho_{Q}\right)^{3} \widetilde{q}(\tau) d\tau \right. \\ &+ \sum_{k=0}^{\infty} \left(\tau_{k} - \rho_{Q}\right)^{3} \Delta \widetilde{Q}\left(\tau_{k}\right) \mathbf{1}_{\left\{0 \leq \tau_{k} \leq T_{R}\right\}} \right]. \end{split} \tag{10}$$

The magnitude of the resilience skewness determines the degree of asymmetry of the recovery with respect to ρ_{O} . Its algebraic sign defines the direction of the skewness. From Equation (10), we can see that $\psi_{O}=0$ when the RDF and RMF are symmetric with respect to ρ_0 . Furthermore, $\psi_{\rm O} > 0$ when the RDF and RMF have longer tails to the right of ρ_O ; and ψ_O < 0 when the left tails of the RDF and RMF are longer. We can interpret $\psi_0 = 0$ as the condition in which the progress in a recovery process has the same pace before and after ρ_O . When ψ_O < 0, the progress is slow during the interval $[0, \rho_0]$ and then it becomes faster over the next period, $(\rho_O, T_R]$. This is the most typical case for recovery processes that include a lengthy planning phase in the post-disruption period. If the planning is done ahead of the disruptive event as a pre-disruption planning and preparation, then we can have $\psi_O > 0$ in which the progress picks up quickly and the relative most time-consuming portion is the actual repair/reconstruction (faster in interval $[0, \rho_0]$) and it slows down over the next interval, (ρ_O, T_R) . We can also define the Relative Resilience Skewness as $\psi_O/T_{R'}^3$ which describes the skewness of the recovery process with respect to the total recovery time, and the Skewness Coefficient as ψ_{O}/χ_{O}^{3} , which describes the skewness of the recovery process with respect to the recovery bandwidth.

As a generalization, we can define the nth Resilience *Moment* as follows:

$$\rho_{Q}^{(n)} := \frac{\int_{0}^{T_{R}} \tau^{n} q(\tau) d\tau}{\int_{0}^{T_{R}} q(\tau) d\tau} = \frac{Q_{\text{res}}}{Q_{\text{tar}}} \rho_{Q,\text{res}}^{(n)} + \frac{\bar{Q}_{\text{res}}}{Q_{\text{tar}}} \rho_{\bar{Q},\text{res}}^{(n)}, (11)$$

where $\rho_{O,res}^{(n)} := \tau_0^n$ and

$$\rho_{\bar{Q},\text{res}}^{(n)} := \frac{1}{\bar{Q}_{\text{res}}} \left[\int_{0}^{T_{R}} \tau^{n} \tilde{q}(\tau) d\tau + \sum_{k=1}^{\infty} \tau_{k}^{n} \Delta \tilde{Q}(\tau_{k}) \mathbf{1}_{\{0 \le \tau_{k} \le T_{R}\}} \right]$$
(12)

The resilience associated with a given system state and a recovery strategy can be completely defined in terms of all its $\rho_O^{(n)}$'s. However, in practice, ρ_O and χ_O might be sufficient to characterize the associated resilience. We can define ρ_O and χ_O as functions of the first two resilience moments as $\rho_Q = \rho_Q^{(1)}$, and $\chi_Q = \sqrt{\rho_Q^{(2)} - \rho_Q^2}$.

As mentioned earlier, there is an analogy between the proposed resilience metrics and equivalent ones in probability theory and mechanics. In particular, ρ_O , χ_O and ψ_O correspond to the mean, standard deviation, and skewness of a random variable when the CRF is replaced with a CDF. Similarly, ρ_O and χ_O are analogous to the centroid and the radius of gyration of the area under $q(\tau)$. Note that, though the proposed resilience analysis is general, the above analogies hold for a non-decreasing CRF.

A closer look to the definitions of R and ρ_0 shows that there are similarities in the way the two metrics quantify resilience. In particular, the following equation shows that ρ_O is an affine function of R:

$$\rho_Q = \frac{\check{Q}(T_R) - R}{\check{Q}(T_R)} \times T_R. \tag{13}$$

Hence, for a given recovery process (i.e. given $\tilde{Q}(T_R)$ and T_p), the information that R provides about resilience is equivalently captured by ρ_O . However, ρ_O can differentiate

Table 2. The proposed resilience metrics, calculated for the recovery curves in Figure 2.

Description	$ ho_{_Q}$	$\chi_{\scriptscriptstyle Q}$
Linear 1	0.25	0.32
Linear 2	0.50	0.65
S-shaped	0.50	0.59

between recovery curves with the same $\check{Q}(T_p)$ but different T_p 's. In addition, R lacks the extra information that the other resilience metrics (e.g. χ_{O} and ψ_{O}) provide. To illustrate this point, we calculate (ρ_{Q}, χ_{Q}) for the three $\check{Q}(\tau)$'s in Figure 2. The results in Table 2 shows that, in contrast to R, the pair (ρ_0, χ_0) can characterize the three different $\dot{Q}(\tau)$'s. Furthermore, a decision-maker can use the $\rho_{O,w}$'s and/or combine ρ_O and χ_O (and, if desired, the higher order moments) to create composite resilience metrics (e.g. $\rho_O \pm \chi_O$ when the two values are in the range $[0, T_R]$).

In practice, the recovery process might be disrupted by shocks at different time instants (see Figure 3). Each shock might cause a sudden reduction in $\check{Q}(\tau)$. The formulation of the resilience moments in Equation (11) accounts for this situation by letting $\Delta \tilde{Q}(\tau_k) < 0$ when a shock occurs at $\tau = \tau_K < T_R$. Alternatively, we can rearrange the terms in Equation (11) to write the overall resilience moments in terms of the set of resilience moments $(\rho_O^{(1)}, \dots, \rho_O^{(n)})_{i'}$ derived for each segment j of $\tilde{Q}(\tau)$ (see Figure 3), that follows the jth shock and before the (j + 1)th shock. Note that we consider τ_i as the reference of the time axis in calculating $(\rho_Q^{(1)},...,\rho_Q^{(n)})_j$. The derived mathematical expression for the overall resilience moments is

$$\rho_{Q}^{(n)} = \sum_{j=0}^{m} \sum_{i=0}^{n} {}^{i}C_{n}\tau_{j}^{n-i}\rho_{Q,j}^{(i)} \times \frac{\breve{Q}\left(\tau_{j+1}^{-}\right)}{\breve{Q}\left(T_{R}\right)} + \sum_{j=0}^{m} \tau_{j}^{n} \frac{\Delta \breve{Q}\left(\tau_{j}\right)}{\breve{Q}\left(T_{R}\right)},\tag{14}$$

where ${}^{i}C_{n} := n!/[i!(n-i)!]$; m is the total number of disrupting shocks; and $\tau_{m+1} := T_R$.

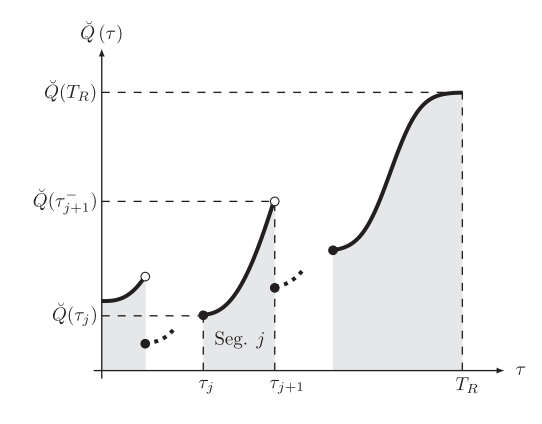


Figure 3. The recovery process might be repeatedly disrupted by shocks.

3. Phases of the recovery process and their role in resilience quantification

In this section, we argue that the different activities in the recovery of engineering systems can generally be grouped into three phases, which we call (1) recovery planning, (2) recovery execution, and (3) recovery closure. Next, we explain how the system state indicators (e.g. reliability and functionality) are affected by the recovery activities and the proposed phases.

3.1. Phases of recovery process

The scope of a recovery process is defined by the magnitude and the nature of the damage sustained by the system. The corresponding recovery process can typically be decomposed into three phases (shown in Figure 4) that we call (1) recovery planning, (2) recovery execution, and (3) recovery closure. These phases can be sequential or overlapping. The recovery planning phase includes the following activities: identification of the objectives of the recovery (i.e. where we want to be at the end of the recovery), development of the recovery strategies (i.e. definition of the activities that will need to take place in order to reach the desired objectives), and securing the required resources for the recovery. The recovery execution phase includes activities where physical progress is made toward achieving the objectives, developed in the recovery planning phase. This phase consumes the majority of the resources (i.e. time, material, and labor). The recovery closure phase involves quality control activities to ensure the recovery completion criteria are met and the system is ready to be put back into operation.

In the specific case of the recovery of a civil structure (e.g. building or bridge) or system/network (e.g. transportation, water, or power network), the three phases

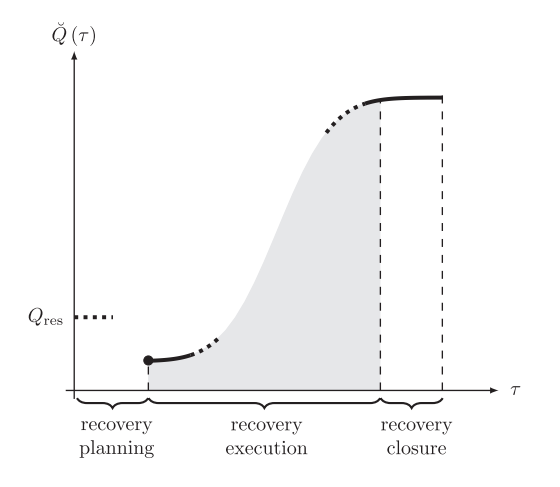


Figure 4. The three phases of the recovery process in the aftermath of a disruption are the (1) recovery planning, (2) recovery execution, and (3) recovery closure.

of the recovery process correspond to what is known in construction management as (1) pre-construction, (2) construction, and (3) post-construction (Klinger & Susong, 2006). The pre-construction phase includes planning, designing, deciding on repair strategies, budgeting financial and other resources, and obtaining work permits from relevant authorities. The construction phase involves physical onsite activities required to repair or replace damaged components. Inspection, quality assurance, safety management, cost and schedule control, and field engineering functions (e.g. onsite decisions) are also activities in this phase. The post-construction phase involves closing activities like the final inspection, handing over, and certification. In mechanical engineering applications such as installation of a new equipment (e.g. a boiler, compressor, or pump), the above three phases correspond to (1) design and planning, (2) mechanical erection, and (3) commissioning. Likewise, when the equipment undergoes a reactive maintenance, the three phases correspond to (1) fault detection, (2) system repairs, and (3) recommissioning.

The duration of each recovery phase depends on the level of damage, the preparedness of the recovery plan, the repairability of the system, and the accessibility of the damaged components. The estimation of the absolute and relative duration of each recovery phase can guide how to expedite the recovery process and improve resilience. For instance, a disaster response plan prepared before a disrupting event strikes can improve resilience by saving valuable time in the recovery planning phase. There might be updates in the planning as new information becomes available during the post-disruption reconnaissance; however, a general planning can be developed ahead of time. Similarly, a well-designed system could favor repairability over constructability to save time in the recovery execution phase.

3.2. Tracking performance indicators during recovery

The phases of the recovery process can be divided into a hierarchy of activities. A work breakdown structure can be designed where activities are further divided up to a required level of detail, based on the functional requirement or available data. The lowest level of activities is where standardized crews, equipment, means, and methods are defined and relevant data are readily available (see, for example, RS Means database (Means, 2008)). Activities in a recovery process have precedence, constraints, and tentative durations associated with them which collectively create a network of activities. Figure 5 shows an example of such a network of recovery activities that is developed for the repair of a damaged RC bridge

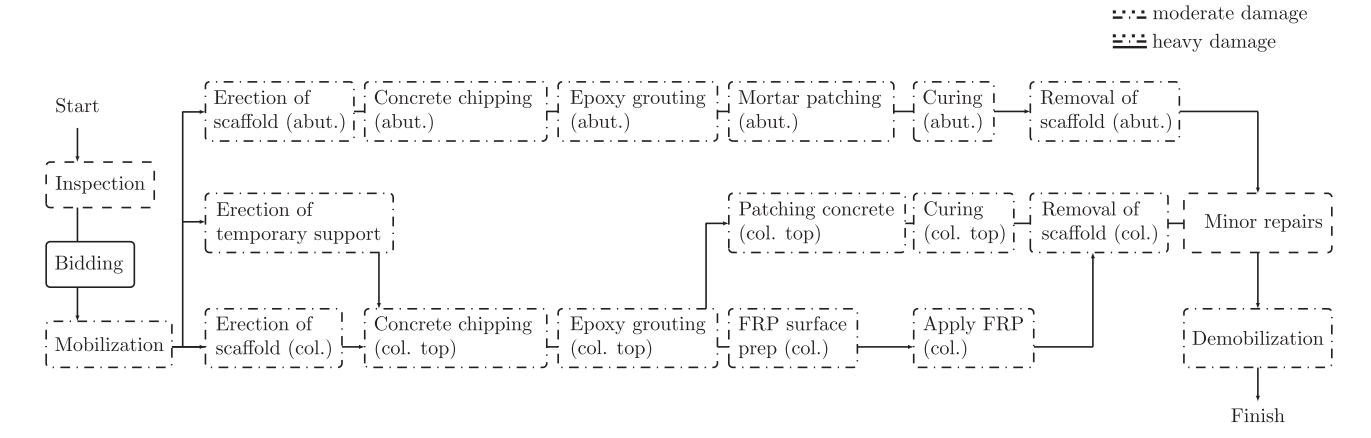


Figure 5. A network of recovery activities developed for the repair of a damaged one single-column bent RC bridge with FRP composites.

with FRP composites. In a typical construction project, the number of activities in the network can be as large as several thousands. Typically, the progress in a construction project is slower at the beginning and toward the end of the project. This is because typically a few activities need to be completed at the beginning before a larger number of activities can be performed in parallel. Toward the end of the project, most of the planned work is completed and only a few activities remain, which might not all be performed in parallel. As a result, the overall work progress gradually decreases until the final completion is achieved.

In a recovery process, work on individual activities might continuously progress over time; however, the changes in the system state occur only at discrete points in time when a group of activities (i.e. a recovery step) is completed. For example, in Figure 5, we consider FRP application (or minor repairs in the case of insignificant damage) as the sole recovery step. The completion time of activities and the corresponding contributions to the system state depend on the activity network, the types of activities, and the metric a decision-maker uses to measure the work progress. For example, one might measure the progress in terms of the expenditure incurred in completing each activity with respect to the total project

expenditure or in terms of activities' contribution to the reliability or functionality of the system. Figure 6 shows a schematic comparison between the work progress in a recovery process and the changes in the reliability and the functionality of a system. The figure illustrates that the work progress might be near-continuous; however, it is only the completion of a group of activities that contributes to the increments in the reliability and in the functionality of the system. The completion of the recovery activities in a group changes both the capacity and the imposed demand on the system and, hence, the reliability (as described in Section 5). Functionality typically has discrete increments when the work completion and the associated reliability reach specific milestones.

· · · · insignificant damage

We can obtain the initial estimates of the durations of individual activities from available databases and past projects. The initial general estimates might need to be updated and tailored to incorporate the effects of influencing factors in a given project such as specific weather conditions, system characteristics, and resource availability. For example, Moselhi, Gong, and El-Rayes (1997) developed a model to estimate the durations of activities, accounting for the impact of weather conditions (temperature, precipitation, wind speed, and humidity). Sukumaran, Bayraktar, Hong, and Hastak (2006)

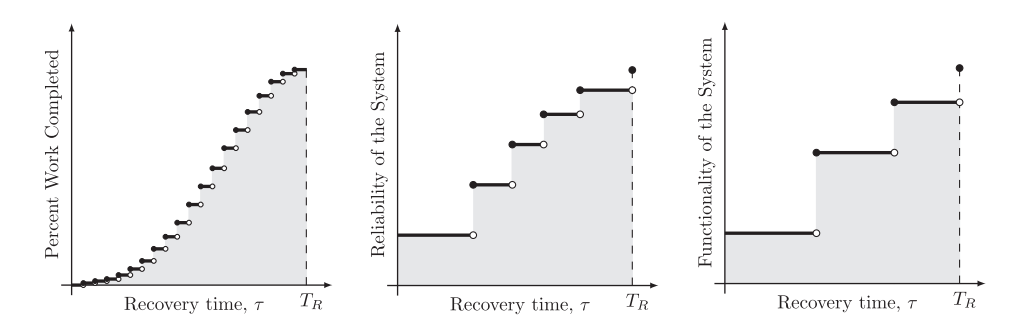


Figure 6. Different performance indicators quantify the recovery progress in dissimilar ways.

identified an extensive list of influencing factors in the case of highway projects and estimated their impact on the durations of activities. Gardoni, Reinschmidt, and Kumar (2007) developed a Bayesian formulation to update the estimate of the future work progress as a function of the work completed up-to-date. While, using more refined models and larger sample sizes can reduce the statistical uncertainty in the estimate of the duration of each individual activity, there remain uncertainties in their values due to the epistemic uncertainty, arising from simplifications in the mathematical models, and aleatory uncertainty, arising from the variability in future conditions (Gardoni, Der Kiureghian, & Mosalam, 2002; Gardoni et al., 2007; Murphy, Gardoni, & Harris, 2011).

For a given system state, we can develop a stochastic network of activities that accounts for the uncertainties in the durations of the individual activities. The stochastic network of activities can then be used to identify the milestones corresponding to the changes in the reliability and functionality of the system and their associated uncertainties.

4. Definition and role of instantaneous reliability

We define the instantaneous reliability as the probability that the system meets a specified performance level at a given time of interest. The higher values of reliability indicate that it is more likely that the system meets the specified performance level. The reliability depends on the state of the system at the considered time and therefore, on the system damage level. Once we obtain the instantaneous reliability of the system, we can find the values of other performance indicators such as damage level and functionality as well as the recovery strategy, which depend on the reliability, as discussed next.

4.1. Definition of damage levels in terms of instantaneous reliability

As discussed in Section 3, to develop the recovery strategy, we need to estimate the extent of damage. Also, when the occurrence of a shock during the recovery disrupts the recovery process, we need to revise the network of recovery activities, based on the new level of damage. The accurate estimation of damage level is particularly important for systems that require a minimum level of safety to resume operation. We define the damage level in terms of the instantaneous reliability of the system to account for the safety considerations and also develop a fully probabilistic formulation for the resilience analysis.

ATC-38 (ATC, 2000) and Bai, Hueste, and Gardoni (2009) define four damage levels based on a qualitative description of the physical damage to a system. Table 3 shows the four damage levels in ATC-38 and the corresponding qualitative descriptions for each damage level. We propose to use definitions of damage levels that are not directly based on the physical damage but based on the implications of such damage on the reliability of the system. The right column of Table 3 provides the definitions of the four damage levels in terms of the reliability of the system. The right column of the table shows that in the proposed reliability-based definition, the four damage levels are delimited by means of three thresholds (i.e. β_0) $\beta_{\rm acc}$, and $\beta_{\rm tol}$). The specification of these thresholds is a system-specific problem. A discussion on the considerations to specify the values of the threshold can be found in Gardoni and Murphy (2014) and Briaud, Gardoni, and Yao (2014).

4.2. Recovery strategy as a function of instantaneous reliability

As shown in Figure 5, in developing the recovery strategy, post-disruption inspection is the first recovery

Table 3. The four damage levels of a system and their descriptions in ATC-38 and the proposed reliability-based definitions.

Damage levels (DLs)	ATC-38 definitions	Proposed reliability-based definitions
None (N)	No damage is visible, either structural or non-structural	The reliability of the system does not change with respect to the reliability of the original system (i.e. $\beta \ge \beta_0$)
Insignificant (I)	Damage requires no more than cosmetic repair. No structural repairs are necessary. For non-structural elements this would include spackling, partition cracks, picking up spilled contents, putting back fallen ceiling tiles, and righting equipment	The reliability of the system decreases but remains above the acceptable threshold (i.e. $eta_{\rm acc} \leq eta < eta_0$). The visible damage to some components triggers the post-disruption inspection
Moderate (M)	Repairable structural damage has occurred. The existing elements can be repaired in place, without substantial demolition or replacement of elements. For non-structural elements this would include minor replacement of damaged partitions, ceilings, contents, or equipment	The reliability of the system decreases below the acceptable threshold but it would be still above a minimum tolerable threshold (i.e. $\beta_{\text{tol}} \leq \beta < \beta_{\text{acc}}$). While, the system does not need to be completely closed, its safety is compromised and the functionality is reduced
Heavy (H)	Damage is so extensive that repair of elements is either not feasible or requires major demolition or replacement. For non-structural elements this would include major or complete replacement of damaged partitions, ceilings, contents, or equipment	The reliability of the system significantly decreases and falls below a minimum tolerable threshold (i.e. $\beta < \beta_{\text{to}}$). So, the damaged components of the system need major repair or complete replacement

activity to determine the extent of damage. The subsequent recovery activities, which are required to achieve a (new) desired system state, are developed in the recovery network based on the assessed damage level. For example, when the inspection results indicate that damage level is insignificant, minor repairs might suffice to achieve the desired state. Alternatively, when the system is moderately damaged, there might be no bidding because the regular maintenance contract of the department of transportation is likely to cover this level of damage. For a heavy damage level, all the recovery activities in the network are needed in order to restore the desired state.

In order to determine the damage level, for developing the network of recovery activities, we use the proposed reliability-based definitions. Furthermore, to incorporate the impact of potential disrupting shocks that might occur during the recovery process, we first determine the new damage level after the occurrence of the shock based on the proposed reliability-based definitions. According to the new damage level, we select a network of recovery activities among the set of networks which are developed a priori for each possible damage level.

4.3. Relation between functionality and instantaneous reliability

There is a relation between the instantaneous reliability of a system and its functionality, as they are both (direct or indirect) functions of the system state. In general, we can distinguish between two cases. In one case, the functionality is defined directly as a function of the system state. So, in this case both the instantaneous reliability of the system and its functionality depend directly on the system state. Water distribution networks are typically analyzed considering this type of dependency (Guidotti et al., 2016). On the other hand, in a fully probabilistic formulation, the functionality is defined by the level of reliability instead of by the level of damage. So, in this case, the instantaneous reliability of the system depends directly on the system state, while the functionality (understood as the functionality of the system on a typical day not considering interruptions due to non-structural reasons) depends on the reliability. This type of dependency is well-suited, for example, when the system requires a minimum level of safety to function (e.g. in the case of buildings and bridges). This type of dependency requires a definition of the damage levels in terms of reliability, as proposed in Table 3.

5. Proposed stochastic formulation of the recovery process

This section explains the proposed formulation for modeling the recovery process, described conceptually in Sections 3 and 4. We model the system state and the corresponding functionality in terms of its instantaneous reliability and as a function of the state variables. The values of the state variables vary with time due to the completion of the recovery steps or the occurrence of disrupting shocks that might occur during the recovery.

5.1. Modeling of the state variables

According to the discussion in Section 3.2, we model the duration of each individual recovery activity as a random variable to account for the uncertainty in their estimates. As a result, the completion times of the *n* recovery steps, $\{\tau_{r,i}\}_{i=1}^n$, form a sequence of random variables. To generate realizations of $\{\tau_{i,i}\}_{i=1}^n$ one can use simulation techniques (e.g. Ditlevsen & Madsen, 1996). The simulation techniques are simple and straightforward but they have three important limitations: (1) as the activity network becomes complex, the number of simulations to capture the uncertainty in $\{\tau_{r,i}\}_{i=1}^n$ increases rapidly and the required simulations become computationally too expensive; (2) the simulation techniques require to repeat the entire set of simulations at future times in order to incorporate any new information, for example, from the completion of some recovery activities or the occurrence of disruptions to the recovery process; and (3) the simulation techniques, in general, do not allow to transfer the information gained from the simulations for one recovery project to other projects.

To address the above limitations, we propose a probabilistic predictive model for the number of completed recovery steps by any time $\tau \in [0, T_R]$ Following the general formulation in Gardoni et al. (2002) for probabilistic models, we write

$$\mathcal{T}\left[\Lambda_r\left(\tau,\boldsymbol{\xi};\boldsymbol{\Theta}_r\right)\right] = \sum\nolimits_{d=1}^{n_d} \theta_{r,d} h_{r,d}(\tau,\boldsymbol{\xi}) + \sigma_r \varepsilon_r, \ \ (15)$$

where $\mathcal{T}(\cdot)$ is a transformation function; $\Lambda_r(\tau, \xi; \Theta_r)$ is the predicted number of completed recovery steps by time τ ; ξ is the set of influencing factors (e.g. weather conditions and resource availability); $\Theta_r = (\theta_r, \sigma_r)$ is a set of unknown model parameters that need to be estimated, in which $\theta_r = (\theta_{r,1}, ..., \theta_{r,n_d}); h_{r,d}(\tau, \xi)$'s are a set of explanatory functions; and $\sigma_r \tilde{\varepsilon_r}$ is an additive model error term (additivity assumption), in which σ_r is the standard deviation of the model error that is assumed to be independent of τ (homoskedasticity assumption) and ε_z is a standard normal random variable (normality assumption). The

choice of $\mathcal{T}(\cdot)$ should be on the basis of satisfying the additivity, homoskedasticity, and normality assumptions as well as increasing the accuracy of the model (i.e. reducing the value of σ_r).

To calibrate the predictive model of $\Lambda_{\cdot}(\cdot)$, one can use an experimental design (Huang, Gardoni, & Hurlebaus, 2010; Tabandeh & Gardoni, 2015) to generate a limited number of samples for $\Lambda_{\cdot}(\cdot)$ and ξ that cover realizations of recovery processes with different topologies of the recovery network and subject to various influencing factors ξ . A Bayesian updating approach (Box & Tiao, 1992; Gardoni et al., 2002) can then be used to estimate Θ_r , based on the generated samples. The developed predictive model of $\Lambda_{\omega}(\cdot)$ is applicable to other recovery projects given that the corresponding topology of the recovery activity network is similar, and the influencing factors are within the range considered in the experimental design.

To model the realizations of $\{\tau_{r,i}\}_{i=1}^n$ we propose a Poisson process with a mean function equal to $\bar{\Lambda}_r(\tau, \xi; \mathbf{\Theta}_r) := \mathbb{E}[\Lambda_r(\tau, \xi; \mathbf{\Theta}_r)]$, where $\mathbb{E}[\cdot]$ is the expected value operator. This is equivalent to modeling the time between the completion of any successive recovery steps, i - 1 and i, with the CDF $F(v) = 1 - \exp\{-[\bar{\Lambda}_r(v + \tau_{r,i-1}) - \bar{\Lambda}_r(\tau_{r,i-1})]\}, \text{ for } v > 0.$

In this model, we can write the PMF of the number of completed recovery steps by any time $\tau \in [0, T_p]$ as

$$\mathbb{P}\left[N_{R}(\tau) = i\right] = \frac{\left[\bar{\Lambda}_{r}\left(\tau, \boldsymbol{\xi}; \boldsymbol{\Theta}_{r}\right)\right]^{i}}{i!} \exp\left[-\bar{\Lambda}_{r}\left(\tau, \boldsymbol{\xi}; \boldsymbol{\Theta}_{r}\right)\right],$$
for $i \in \{0, 1, \dots, n\},$

$$(16)$$

where n is the total number of recovery steps.

The completion of each recovery step corresponds to reaching a milestone for which the desired values of the state variables, $\mathbf{X}(\tau_{r,i})$, are known (typically, in a probabilistic sense). Note that the recovery process may introduce new variables to $\mathbf{X}(\tau_{r,i})$ or replace a subset of variables in $\mathbf{X}(\tau_{r,i})$ with new ones. For example, if a retrofit is implemented using FRP composites, $\mathbf{X}(\tau_r)$ will include new variables that define the FRP and/or its properties.

The recovery process ends when all the steps in the original recovery network are completed (i.e. $N_R(T_R) = n$), given that no disrupting shock occurs. When the occurrence of a shock disrupts the recovery process, we have to re-estimate the number of remaining recovery steps, their completion times, and the values of the state variables after each of the remaining recovery steps. As described conceptually in Section 4, we have to first determine the damage level based on the reliability of the system. Because the reliability is a function of state variables, we

need to determine the impact of the shock on the state variables.

The occurrence of disrupting shocks is typically modeled as a Poisson or a renewal process. For example, to model the occurrence of earthquake mainshocks, it is common to use a homogeneous Poisson process or, more generally, a renewal process (Takahashi, Der Kiureghian, & Ang, 2004; Yeo & Cornell 2009a). The occurrence of earthquake aftershocks is typically modeled as a non-homogeneous Poisson process (Jia, Tabandeh, & Gardoni, 2017; Kumar & Gardoni, 2014a).

Given the occurrence of a disrupting shock, we use the general formulation proposed by Jia and Gardoni (2017a) to model the impact on the state variables. We write the vector of state variables as $\mathbf{X}(\tau_{s,i}) = \mathbf{X}(\tau_{s,i}^-) + \Delta \mathbf{X}(\tau_{s,i})$, where $\mathbf{X}(\tau_{s,i}^{-})$ is the vector of state variables immediately before the occurrence of the *j*th shock and $\Delta \mathbf{X}(\tau_{s,i})$ is the change in the state variables due to the jth shock. In general, $\Delta \mathbf{X}(\tau_{s,j})$ is a function of $\mathbf{X}(\tau_{s,j}^{-})$ and the intensity of the shock, $S(\tau_{s,i})$. To account for such dependence, one can develop/adopt probabilistic predictive models for $\Delta \mathbf{X}(\tau_{s,i})$ (see Jia & Gardoni, 2017b; Kumar & Gardoni, 2012, 2014b). We denote the set of parameters of such models as $\Theta_{\mathbf{x}}$. Note that the inclusion of $\mathbf{X}(\tau_{s,i}^-)$ in predict- $\operatorname{ing} \Delta \mathbf{X}(\tau_{s,i})$ accounts for the fact that the imposed changes are state-dependent (i.e. the impact of a given shock on the state variables depends on the most recent values of the state variable).

Combining the effects of the recovery process and disrupting shocks, we can write the state variables at any time $\tau \in [0, T_p]$ as

$$\mathbf{X}(\tau) = \sum_{i=1}^{\infty} \mathbf{X}(\tau_{r,i-1}) \mathbf{1}_{\{\tau_{r,i-1} \le \tau < \tau_{r,i}\}}$$

$$+ \sum_{i,j=1}^{\infty} \Delta \mathbf{X}(\tau_{s,j}) \mathbf{1}_{\{\tau_{r,i-1} < \tau < \tau_{r,i}, \tau_{r,i-1} < \tau_{s,j} \le \tau\}}.$$

$$(17)$$

The probability distributions of the state variables at the beginning of the recovery process ($\tau = 0$) can be obtained from the deterioration modeling (Iervolino, Giorgio, & Polidoro, 2015; Jia & Gardoni, 2017a; Jia et al., 2017). For the subset of state variables which are new or replaced during the recovery process, the initial probability distributions are determined in compliance with the objective(s) of the recovery (e.g. to restore the original reliability or functionality of the system or achieve a higher one, if desired).

5.2. Stochastic capacity and demand models

To model the capacity and demand of the system, we use the predicted value of $\mathbf{X}(\tau)$ in existing capacity and demand models. The general expression for the capacity of a system can be written as

$$C(\tau) := C[\mathbf{X}(\tau); \mathbf{\Theta}_C], \tag{18}$$

where $C[\mathbf{X}(\tau); \mathbf{\Theta}_C]$ is the predicted capacity of the system at time $\tau \in [0, T_R]$ and Θ_C is a set of parameters of the capacity model. Similarly, we can write the following general expression for the demand that a shock with intensity measure(s) $S(\tau)$ can impose on the system:

$$D(\tau) := D[\mathbf{X}(\tau), \mathbf{S}(\tau); \mathbf{\Theta}_{D}], \tag{19}$$

where $D[\mathbf{X}(\tau), \mathbf{S}(\tau); \mathbf{\Theta}_{D}]$ is the predicted demand on the system at time $\tau \in [0, T_R]$ and Θ_D is a set of parameters of the demand model. For example, one can use the capacity models in Gardoni et al. (2002) and the demand models in Gardoni, Mosalam, and Der Kiureghian (2003) or Huang et al. (2010) for RC bridges. Also, Tabandeh and Gardoni (2014, 2015) developed probabilistic capacity and demand models for RC bridges, retrofitted with FRP composites.

5.3. Instantaneous reliability

Using the capacity and demand models in Equations (18) and (19), we can write the limit-state func $g(\tau) = C(\tau) - D(\tau),$ as where the $\{[\mathbf{X}(\tau), \mathbf{S}(\tau)]: g(\tau) \leq 0\}$ defines the failure to meet a specified performance level. We can write the conditional failure probability (i.e. fragility) at any time $\tau \in [0, T_R]$ given the occurrence of a shock with an intensity $S(\tau)$ as $\mathcal{F}[S(\tau);\Theta] := \mathbb{P}[g(\tau) \leq 0|S(\tau)]$, where $\Theta = (\Theta_{\mathbf{v}}, \Theta_{\mathbf{r}}, \Theta_{\mathbf{C}}, \Theta_{\mathbf{D}})$. According to Gardoni et al. (2002), there are two possible ways to incorporate the uncertainty in Θ when computing $\mathcal{F}[S(\tau); \Theta]$. First, we may ignore the uncertainty in Θ and obtain a point estimate of the fragility as $\hat{\mathcal{F}}[\mathbf{S}(\tau)] := \mathcal{F}[\mathbf{S}(\tau); \hat{\mathbf{\Theta}}]$, where $\hat{\mathbf{\Theta}}$ is a fixed value of Θ (e.g. the mean value). Alternatively, we can account for the uncertainty in Θ to obtain a predictive estimate of the fragility as $\tilde{\mathcal{F}}[\mathbf{S}(\tau)] = \int \mathcal{F}[\mathbf{S}(\tau); \mathbf{\Theta}] f(\mathbf{\Theta}) d\mathbf{\Theta}$, where $f(\mathbf{\Theta})$ is the PDF of $\mathbf{\Theta}$.

Given the fragility function at τ , $\mathcal{F}[\mathbf{S}(\tau)]$ (i.e. $\hat{\mathcal{F}}[\mathbf{S}(\tau)]$ or $\mathcal{F}[\mathbf{S}(\tau)]$), we can write the instantaneous failure probability, $\mathcal{P}_f(\tau)$, as

$$\mathcal{P}_{f}(\tau) = \int \mathcal{F}[\mathbf{S}(\tau)] f[\mathbf{S}(\tau)] d\mathbf{S}(\tau), \tag{20}$$

where $f[\mathbf{S}(\tau)]$ is the PDF of $\mathbf{S}(\tau)$. Using $\hat{\mathcal{F}}[\mathbf{S}(\tau)]$ in Equation (20), we obtain a point estimate of the failure probability (i.e. $\hat{\mathcal{P}}_f(\tau)$). Alternatively, using $\tilde{\mathcal{F}}[\mathbf{S}(\tau)]$, we obtain a predictive estimate of the failure probability (i.e. $\mathcal{P}_f(\tau)$). The instantaneous reliability is simply $\mathcal{R}(\tau) = 1 - \mathcal{P}_f(\tau)$ and the corresponding instantaneous reliability index is

 $\beta(\tau) = \Phi^{-1}[\mathcal{R}(\tau)]$, where $\Phi(\cdot)$ is the standard normal CDF. Similarly, we can define $\beta(\tau, \mathbf{S}) = \Phi^{-1} \{ \mathcal{R}[\mathbf{S}(\tau)] \}$, where $\mathcal{R}[\mathbf{S}(\tau)] = 1 - \mathcal{F}[\mathbf{S}(\tau)].$

5.4. System functionality

When the system functionality is directly defined in the terms of the system state, system functionality can be calculated in parallel with the instantaneous reliability, by taking into account any recovery steps or disrupting events, which may affect the system state. Such a procedure is similar to the one we described in Section 5.3.

When the functionality is defined by the level of reliability (like for buildings and bridges) the different states of functionality are typically specified according to the requirements of stakeholders or community to meet different operation levels. In such a case, we need to develop a mapping function $\mathcal{M}:[0,1]\times\mathbb{T}\mapsto [0,100]$ which determines the system functionality at any time instant $\tau \in \mathbb{T}$ in terms of $\mathcal{R}(\tau) \in [0, 1]$. The properties of \mathcal{M} such as being continuous or discrete and the number of possible states in the case of discrete functionality need to be defined for the specific system under study. For example, in a bridge system when $\beta_{\text{tol}} \leq \beta(\tau) < \beta_{\text{acc}}$, the traffic load might need to be reduced which means reduction in the functionality with respect to the intact system. The amount of reduction in the functionality of an interstate bridge could be specified by the department of transportation. Also, when $\beta(\tau) < \beta_{\text{tol}}$, the bridge need to be closed to the traffic because of safety considerations and, thus, the system functionality becomes zero.

6. Estimation of recovery quantifiers

Various quantities can be defined to describe the recovery process (which we call recovery quantifiers). Such recovery quantifiers can be used in life-cycle analysis (Jia et al., 2017; Kumar & Gardoni, 2014a). The recovery quantifiers can also serve as basis to predict and compare the system performance for different design and operation strategies. Some of the useful recovery quantifiers that can be derived from the proposed formulation are (1) the amount of progress by any given time, in terms of the instantaneous reliability and system functionality; (2) the amount of required work, in terms of the number of recovery steps; (3) the level of risk involved, in terms of the number of shocks that might occur during the recovery process; (4) the system down/partial functionality time, in terms of the recovery duration; and (5) the resilience of the system, in terms of the proposed resilience metrics.

The instantaneous reliability is the recovery quantifier which is also used to compute the other recovery quantifiers. To calculate the instantaneous reliability, we solve Equation (20) at time instants at which changes occur in the reliability of the system (Figure 6). We follow two main steps: (1) we simulate the occurrence time of the events that affect the reliability of the system (i.e. recovery steps and disrupting shocks), and (2) we calculate the reliability of the system after each event.

To simulate the occurrence times, we first set a time horizon, τ_{HP} over which we perform the calculations. Next, we simulate the completion times of the recovery steps using a general non-homogeneous Poisson process with a mean function given in Equation (15) and conditioned on the event $N_R(T_R) = n$. We use the following algorithm to simulate $\{\tau_{r,i}\}_{i=1}^n$:

Algorithm 1 Simulation of the completion times of the recovery steps

```
1: draw n independent copies of \tau_{\pi(i)} \sim \Lambda_r(\cdot; \Theta_r)/n

2: set (\tau_{r,1}, \dots, \tau_{r,n}) = \operatorname{sort}(\tau_{r,\pi(1)}, \dots, \tau_{r,\pi(n)})

3: set k = \max\{i: \tau_{r,i} \leq \tau_{H}\}

4: accept (\tau_{r,1}, \dots, \tau_{r,k})
```

where $\pi(\cdot)$ is a permutation operator such that $\pi(1), ..., \pi(n)$ is a reordering of 1, ..., n; $\Lambda_r(\cdot; \mathbf{\Theta}_r)/n$ is the conditional CDF of the completion times of the recovery steps; and $k \in [0, 1, ..., n]$ is the total number of recovery steps that are completed within the specified time horizon.

Next, we simulate the sequence $\{\tau_{s,j}\}_{j=1}^m$ such that $\tau_{s,m} \leq \tau_H$. Assuming that disrupting shocks are occurring according to a general non-homogeneous Poisson process with a mean function $\Lambda_s(\tau) = \int_0^\tau \lambda_s(v) dv$ such that $\lambda_s(\tau) \leq \lambda_{s,ub}$ for all $\tau \in [0, \tau_H]$, we use the following algorithm to simulate $\{\tau_{s,i}\}_{i=1}^m$:

Algorithm 2 Simulation of the occurrence times of disrupting shocks

```
1: set \tau_{s,0} = 0

2: while \tau_{s,j} < \tau_H do

3: draw a sample for the interarrival time d_{sj} \sim Exp(\lambda_{s,ub})

4: set \tau_{sj} = \tau_{s,j-1} + d_{sj}

5: draw a random number u \sim U(0, 1)

6: if \lambda_s(\tau) < \lambda_{s,ub}

7: reject \tau_{s,j} and go to step 3

8: else

9: accept \tau_{s,j}

10: end
```

In the above algorithm, $d_{s,j}$ is the interarrival time between subsequent shocks (j-1) and j.

In the second step, to calculate the instantaneous reliability of the system, we consider two cases: (1) $\tau_{r,k} < \tau_{s,1}$ and (2) $\tau_{r,k} > \tau_{s,1}$. In the first case, the recovery process

ends before the occurrence of any disrupting shocks. As a result, we can solve Equation (20) as k time-invariant reliability problems, using the common approaches of reliability analysis (see, for example, Ditlevsen & Madsen, 1996; Gardoni, 2017). In the second case, only a subset (possibly empty) of the recovery steps is completed before the occurrence of the first disrupting shock at $\tau_{s,t}$. Now, we calculate the reliability of the system in the same way as explained for the first case but considering only the subset of recovery steps. For the subset of recovery steps which are not completed by $\tau_{s,t}$, we have to revise the original network of recovery activities based on the new damage level at $\tau_{s,t}$. To determine the new damage level according to the proposed reliability-based definition, we have to obtain $\beta(\tau_{s,1})$. To this end, we draw a sample from the probability distribution of $S(\tau_{s,1})$ and use it together with $\mathbf{X}(\tau_{s_1}^-)$ in the probabilistic predictive models of $\Delta\mathbf{X}(\tau_{s_1})$. Next, we estimate the state variables at time $\tau_{s,1}$, $\mathbf{X}(\tau_{s,1})$, according to Equation (17). Using the estimated $\mathbf{X}(\tau_{s,1})$, we can write the limit-state function and solve Equation (20) to obtain $\mathcal{R}(\tau_{s,1})$. Using $\beta(\tau_{s,1}) = \Phi^{-1}[\mathcal{R}(\tau_{s,1})]$, we can determine the new damage level according to Table 3. Finally, we select the corresponding network of recovery activities, developed a priori for the new damage level. The calculation of the instantaneous reliability continues in the same way, until either the recovery process ends (i.e. all the determined recovery steps all completed). In this algorithm τ_H should be sufficiently big so that the recovery process ends before τ reaches τ_H .

The above two steps explain the simulation of the instantaneous reliability at any time τ conditional on $\{\tau_{r,i}\}_{i=1}^n$, $\{\tau_{s,j}\}_{j=1}^m$, and $\{\mathbf{S}(\tau_{s,j})\}_{j=1}^m$. To obtain the unconditional instantaneous reliability, we need to repeat the above two steps for different realizations of $\{\tau_{r,i}\}_{i=1}^n$, $\{\tau_{s,j}\}_{j=1}^m$, and $\{\mathbf{S}(\tau_{s,j})\}_{j=1}^m$. We can use the statistical average of the simulated instantaneous reliabilities as an estimator of the unconditional instantaneous reliability. The number of required simulations is determined such that the coefficient of variations (COVs) of the calculated statistical averages at all times $\tau \in [0, \tau_H]$ are less than a prescribed threshold (e.g. COV = 0.05).

The computational time of the simulations depends on the complexity of (1) the occurrence modeling of the recovery steps and disrupting shocks, and (2) the resultant impact on the state variables. Using the analytical predictive models as proposed in Equations (15)–(19), a naïve implementation of the formulation is efficient enough to run on a typical personal computer.

We use the simulated realizations of the instantaneous reliability to estimate the other recovery quantifiers: N_R , N_S , T_R , and the resilience metrics. In each realization of the instantaneous reliability, the corresponding total number of completed recovery steps, n, the number of disrupting

shocks, m, and the completion time of the last recovery step, $\tau_{r,n}$, are realizations of N_R , N_S , and T_R , respectively. We can use the obtained realizations of N_p , N_s , and T_p to approximate the corresponding probability distributions, based on a probability estimation approach (e.g. Bishop, 2006)

To quantify the system resilience, we can select a set of resilience metrics from the ones defined in Equations (7)–(11). We can use the realizations of the instantaneous reliability in the respective equations to obtain the corresponding realizations of the reliability-based resilience metrics. We can then use these realizations to obtain the respective statistics of the resilience metrics, similar to the other recovery quantifiers. When the resilience is in terms of the system functionality, we can obtain the functionality-based resilience metrics by first obtaining the realizations of the system functionality by applying the mapping function \mathcal{M} to the realizations of the instantaneous reliability and then proceeding as for the estimation of the reliability-based resilience metrics.

7. Illustrative example

This section illustrates the proposed formulation considering the resilience analysis of an example RC bridge subject to seismic excitations. Figure 7 shows the configuration of the considered (single column, single bent) bridge together with the schematic layout of the considered site. The details of the considered bridge can be found in Kumar and Gardoni (2014a) and Jia et al. (2017). For the purpose of the recovery of the example bridge, we consider a repair strategy with FRP composites based on Saini and Saiidi (2013).

To model the impact of the recovery process and disrupting shocks on the system state, we consider both the impact on the state variables as well as the resulting impact on the structural properties. Specifically, the recovery process introduces new state variables which are the properties of the FRP composites, including thickness,

tensile strength, and Young's modulus. Furthermore, we consider the impact on the structural properties, including the ultimate curvature capacity of the RC section, ϕ_{ν} , the pre-yield lateral stiffness of the RC column, K, and the yield displacement of the RC column, Δ_{v} . Modeling the structural properties is convenient as we use them directly in the probabilistic capacity and demand models discussed later.

To determine the damage levels, we use the reliability-based definitions in Table 3. For this example, we assume the following values for the reliability thresholds: $\beta_0 = 3.5$, $\beta_{\rm acc} = 2.5$, $\bar{\beta}_{\rm tol} = 1.5$. We also define the following mapping function $\mathcal M$ between the instantaneous reliability and the system functionality:

$$\mathcal{M} = \begin{cases} 0\%, & \beta < \beta_{\text{tol}}, \\ 30\%, & \beta_{\text{tol}} \le \beta < \beta_{\text{acc}}, \\ 70\%, & \beta_{\text{acc}} \le \beta < \beta_{0}, \\ 100\%, & \beta \ge \beta_{0}. \end{cases}$$
 (21)

7.1. Recovery process and the impact on the system

For this example, we use the network of recovery activities already shown in Figure 5. Table 4 shows the durations of the individual recovery activities, obtained from the RS Means database (Means, 2008) and similar projects (Saini & Saiidi, 2013). In addition to the most likely durations of the individual activities, the table reports the lower and upper bounds of the durations that represent the variability in their estimates. The table also shows the set of predecessors of each activity (recovery activities needed before a specific activity can start). We need the information on the predecessors to estimate the completion times of the recovery steps. In this example, because there is only one recovery step, the completion time of the recovery step is the completion time of the recovery process (i.e. $\tau_{r,1} = T_R$).

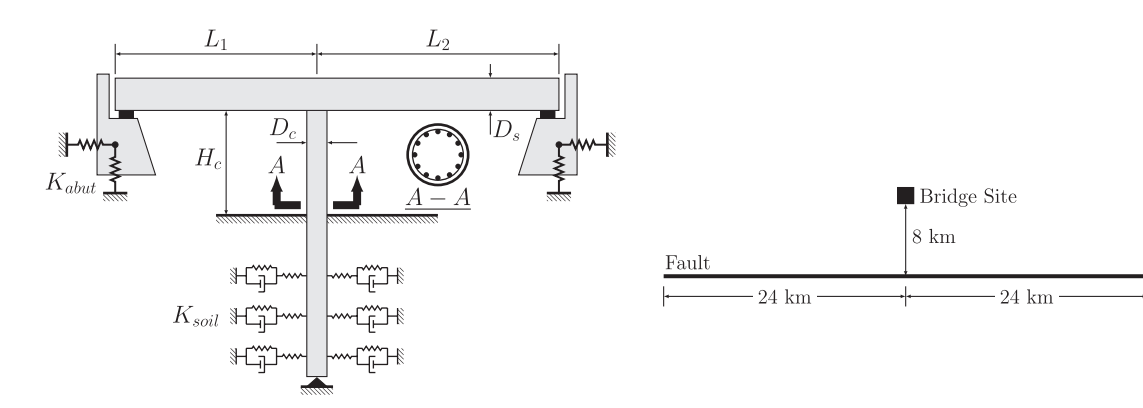


Figure 7. The considered RC bridge and layout of the hypothetical site (adapted from Jia et al., 2017).



Table 4. The time table of the recover	vactivities for the repair of the da	maged RC bridge with FRP composites.
Table 4. The time table of the recover	v activities for the rebail of the da	illaded Ne bildde with i Ni Collibosites.

	Activity	Duration (days)			
Number		Lower bound	Most likely	Upper bound	Predecessor(s)
1	Inspection	2	3	5	
2	Bidding	15	20	30	1
3	Mobilization	5	7	15	2
4	Erection of scaffold (abutment)	1	2	3	3
5	Erection of temporary support	1	2	3	3
6	Erection of scaffold (pier)	1	2	3	3
7	Concrete chipping (abutment)	1	2	3	4
8	Epoxy grouting (abutment)	1	2	3	7
9	Mortar patching (abutment)	1	2	3	8
10	Curing (abutment)	7	10	15	9
11	Removal of scaffold (abutment)	1	2	3	10
12	Concrete chipping (pier top)	1	2	3	4 and 5
13	Epoxy grouting (pier top)	2	3	3	12
14	Patching concrete (pier top)	1	2	3	13
15	Curing (pier top)	7	10	15	14
16	FRP surface prep (pier)	0.5	1	2	15
17	Apply FRP (pier)	0.5	1	2	16
18	Removal of scaffold (pier)	0.5	1	2	15 and 17
19	Minor repairs	3	4	5	11 and 18
20	Demobilization	0.5	1	2	19

We model the duration of each individual recovery activity as a random variable with a Beta distribution, according to the information in Table 4. We then use stochastic activity network scheduling techniques (Duncan, 1996) to estimate τ_r , based on the samples of the durations of the individual recovery activities. Table 5 shows the estimated distribution parameters for $\tau_{r,1}$ in different recovery projects corresponding to the different levels of damage. As discussed in Section 5.1, for the complex networks of recovery activities with large numbers of recovery steps (i.e. large *n*), it is more convenient to first develop a model for $\Lambda_{\cdot}(\cdot)$, following the general expression in Equation (15), and then use the Poisson process as in Equation (16) to generate realizations of $\{\tau_{r,i}\}_{i=1}^n$.

The recovery process affects the system state by adding the FRP properties (i.e. thickness, tensile strength, and Young's modulus) to the set of state variables. The recovery process also affects the structural properties ϕ_{μ} and Δ_{μ} (but not *K*), the extent of which depends on the properties of the FRP composites. The properties of FRP composites can be selected to achieve the desired state of the system (e.g. in terms of target reliability). In this example, we set the target reliability after the completion of the repair to be 10% higher than the reliability of the original as-built bridge. One can use the capacity model in Tabandeh and Gardoni (2014) and the demand model in Tabandeh and Gardoni (2015) to formulate a reliability-based search problem and obtain the values of the FRP properties.

7.2. Disrupting shocks and the impact on the system state

In this example, we consider the earthquake mainshocks and the following aftershocks as the potential disrupting events that might occur during the recovery process. To

Table 5. The estimated parameters of Beta distributions for τ_{r_1} corresponding to the three damage levels.

	 Range of Beta dis- 		
Damage Levels	α	β	tribution (days)
I	5.29	6.78	[5,10]
М	7.36	9.38	[19,34]
Н	8.36	13.78	[40,77]

model $\{\tau_{s,i}\}_{i=1}^m$ we use a homogeneous Poisson process for the occurrence of the earthquake mainshocks and a non-homogeneous Poisson process for the occurrence of the earthquake aftershocks. The details of modeling the occurrence of earthquake mainshock-aftershocks sequence can be found in Jia et al. (2017).

In order to determine the impact of a disrupting shock on the systems state, we need to estimate the intensity of the shock. In this example, we use the spectral acceleration, S_a , as the intensity measure. To obtain the PDF of S_a , we need to perform a probabilistic seismic hazard analysis for the mainshock-aftershocks sequence. The details of the seismic hazard analysis can be found in Kramer (1996) and Yeo and Cornell (2009b). For a given value of S_a , we use the probabilistic models developed by Kumar and Gardoni (2014b) to predict the degradation of ϕ_{ij} , K, and Δ_{ij} . The details on the state-dependent models can be found in Jia and Gardoni (2017b). Once we obtain the values of ϕ_{ν} , K, and Δ_{ν} , we use them in the probabilistic capacity model developed by Gardoni et al. (2002) and the demand model developed by Gardoni et al. (2003) to write the limit-state function and then calculate the instantaneous reliability, as explained in Section 6.

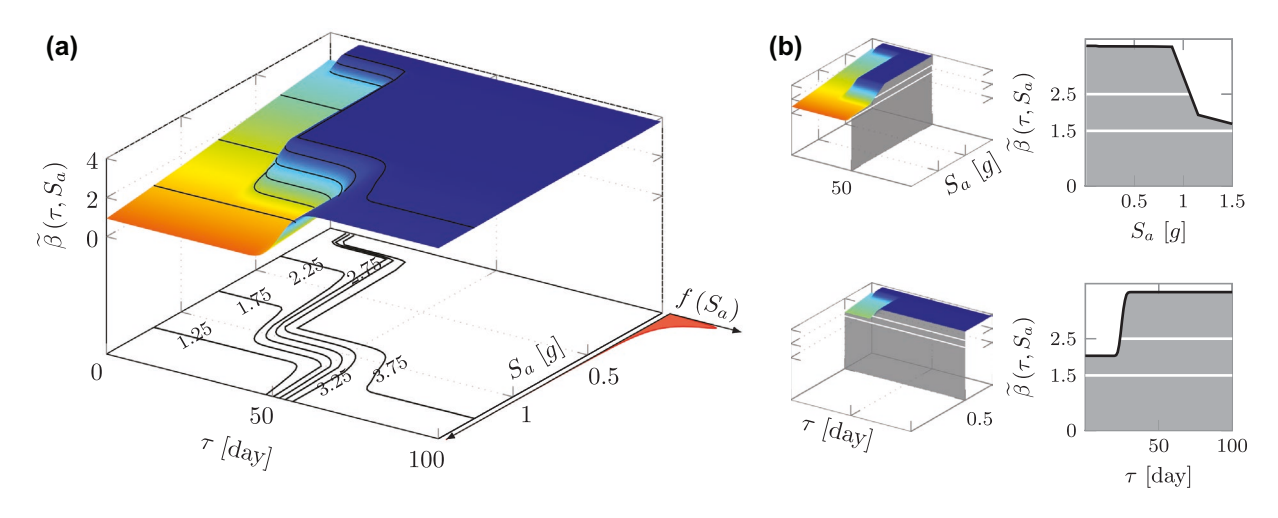


Figure 8. The (a) recovery surface and (b) recovery curve of the example RC bridge in terms of predictive reliability index.

7.3. Results and discussion

In this example, we used COV = 0.05 of the instantaneous reliability index as the convergence criterion, which required approximately 10,000 simulations of $\{\tau_{r,i}\}_{i=1}^n$, $\{\tau_{s,j}\}_{j=1}^m$, and $\{\mathbf{S}(\tau_{s,j})\}_{j=1}^m$. The analysis took approximately 10 min of runtime on a personal computer (Intel(R) core(TM) i5-4460 CPU @ 3.20 GHz with 8.00 GB RAM).

Figure 8(a) shows the recovery surface in terms of the predictive reliability index, $\tilde{\beta}(\tau, S_a)$, and the PDF of S_a , $f(S_a)$, where S_a is the intensity measure of the earthquake after which the recovery process starts. Furthermore, to explore the impact of S_a on the recovery process and the progress over time for a given S_a , Figure 8(b) shows the curves $\tilde{\beta}(\tau=50,S_a)$ and $\tilde{\beta}(\tau,S_a=0.5)$. The white lines indicate the locations of $\beta_{\rm tol}=1.5$ and $\beta_{\rm acc}=2.5$. For small values of S_a (i.e. $S_a \in [0,0.1]$), the initial damage level of the system is insignificant and the system quickly recovers up to the desired value, with a mean recovery time of $\mathbb{E}[T_R] \approx 7$ days. For intermediate values of S_a (i.e. $S_a \in [0.1,0.9]$), the initial damage level is moderate and

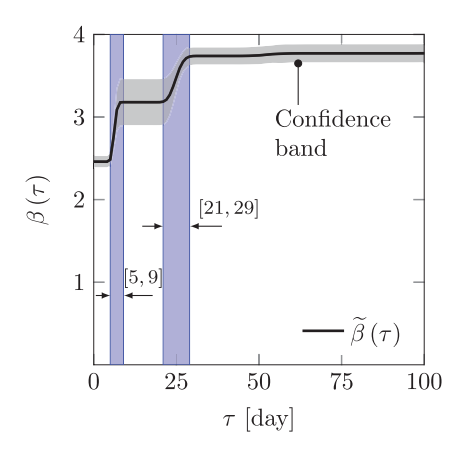


Figure 9. The recovery curve of the example RC bridge in terms of the predictive instantaneous reliability index.

the corresponding recovery time is longer than that for the small values of S_a , with a mean recovery time of $\mathbb{E}[T_R] \approx 26$ days. For large values of S_a (i.e. $S_a \in [0.35\,g, 1.5\,g]$), the initial damage level is heavy and the corresponding recovery time has the mean $\mathbb{E}[T_R] \approx 54$ days. Having three discrete damage levels creates these three trends over time.

Figure 9 shows the recovery curve in terms of the predictive instantaneous reliability index, $\tilde{\beta}(\tau)$. The figure also shows the confidence band (between $\tilde{\beta}(\tau) - \sigma_g(\tau)$ and $\tilde{\beta}(\tau) + \sigma_{\theta}(\tau)$) due to the statistical uncertainty in Θ . We can observe that most of the recovery progress occurs over two distinct intervals, $\tau \in [5, 9]$ and $\tau \in [21, 29]$. To explain this observation, we note that the initial damage level is a function of $\tilde{\beta}(\tau = 0)$ which is obtained using Equation (20) considering $\tilde{\beta}(\tau = 0, S_a)$ instead of $\mathcal{F}[\mathbf{S}(\tau)]$. In this example, $\beta(\tau = 0, S_a)$ is such that for the most likely values of S_a , the initial damage could be either insignificant or moderate. When the initial damage level is insignificant, the recovery time is in the first of the two intervals with probability $\mathbb{P}(T_R \in [5, 9] | DL = I) = 0.997$. On the other hand, when the initial damage level is moderate, the probability that the recovery process ends within the second interval is $\mathbb{P}(T_R \in [21, 29]|DL = M) = 0.954$ We can also observe that the confidence band is larger in the interval $\tau \in [9, 21]$ due to the various possible recovery trends, which are highly sensitive to the initial damage level.

Figure 10 shows the PDF and PMF of the recovery quantifiers T_R (Figure 10(a)), and N_S (Figure 10(b)). In this example, because there is only one recovery step, $\mathbb{P}(N_R=1)=1$. Figure 10(a) also shows the conditional PDFs of T_R , $f_{T_R|DL}(\tau|DL)$, for three different initial damage levels, considering that no disrupting shock occurs during the recovery (i.e. the PDFs in Table 5). We can observe that $f_{T_R}(\tau)$ in this example is bimodal. This is because, as explained earlier, the initial damage level of the example bridge could be either insignificant or moderate with

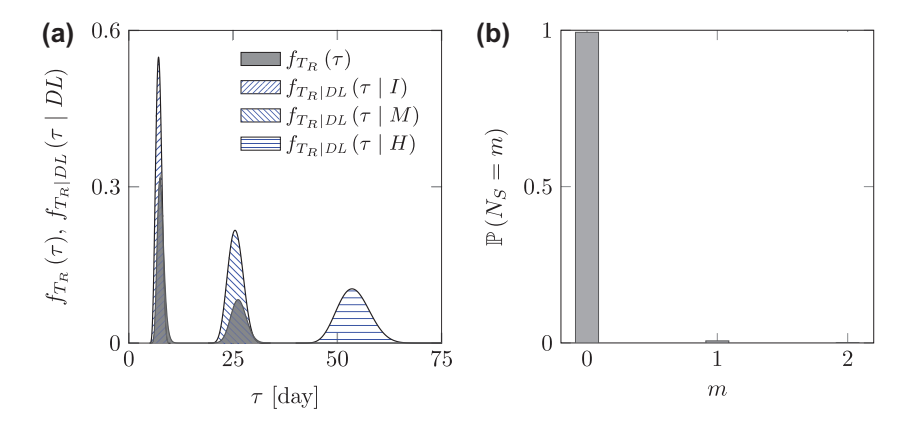


Figure 10. The PDF and PMF of the (a) recovery time, and (b) number of disrupting shocks during the recovery process.

comparable probabilities (while the probability of being heavy is negligible). Due to the occurrence of disrupting shocks, we also observe that the peaks of $f_{T_R}(\tau)$ for example, bridge shift toward higher values of τ with respect to the modes of $f_{T_R|DL}(\tau|DL)$ for insignificant and moderate initial damage levels.

In Figure 10(b), we observe that $\mathbb{P}(N_S = m)$ is concentrated at m = 0, and decreases significantly for higher values of m. This is because the mean return period of seismic shocks (\approx 6 years) is significantly larger than the expected completion time of the recovery process (\approx 16 days); thus, it is unlikely that an earthquake would disrupt the recovery process.

We use the instantaneous reliability and the system functionality as the performance indicators to estimate the reliability- and functionality-based resilience metrics of the example bridge. To obtain the system functionality, we use the mapping function $\mathcal M$ defined in Equation (21). Table 6 summarizes the estimated statistics of the reliability- and functionality-based resilience metrics ρ_Q , χ_Q , and $\psi_Q^{1/3}$. The values of the standard deviations for ρ_Q , χ_Q , and $\psi_Q^{1/3}$ are large (with respect to the mean values). This is due to the effect of the initial damage level on the recovery process. Comparing the resilience metrics based on the two performance indicators, we observe that the mean values of the functionality-based resilience metrics are larger than the reliability-based metrics. This is because the scale of variation, as defined by $\bar{Q}_{\rm res}/Q_{\rm tar}$, of the system functionality is higher than that of the

Table 6. The statistics of reliability- and functionality-based resilience metrics.

	Reliability-based		Function	ality-based
Resilience metric	Mean	Standard deviation	Mean	Standard deviation
$\overline{ ho_Q}$	0.29	1.95	9.36	11.27
χ_{0}	1.58	2.62	4.23	3.12
$\chi_Q = \chi_Q^{1/3}$	3.28	4.04	4.74	3.31

instantaneous reliability. For example, with reference to Equation (8), we note that in ρ_O the value of $\rho_{\bar{O},res}$ (=16.5) is the same for the reliability- and functionality-based metrics. However, the value of \bar{Q}_{res}/Q_{tar} in the reliability-based metric (=0.006) is significantly smaller than that of the functionality-based metric (=0.468). Furthermore, we observe that the differences among the reliability- and functionality-based metrics diminishes as the order of the metrics increases (e.g. the difference between the two χ_0 's is less than that of ρ_0 's). This is because increasing the order of the resilience metric, increases the effect of the recovery trend (determined by the time instants when a change in the system state occurs) on the resilience metric, as compared to the effect of the scale of variation in the performance indicator. The recovery trend is similar for both the reliability- and functionality-based metrics; thus, the difference between the corresponding resilience metrics decreases with increase in the order of the resilience metric. These observations indicate (1) the importance of considering functionality in addition to reliability (i.e. considering functionality-based resilience metrics instead of only reliability-based resilience metrics); and (2) the importance of choosing the metrics of interest and interpreting/communicating the obtained results.

8. Conclusion

This paper proposed a rigorous mathematical formulation to quantify the resilience of engineering systems. Proposed resilience metrics can accurately quantify the resilience of a given engineering system and differentiate between various resilient characteristics of any two systems. Resilience metrics constitute a systematically expandable set of partial descriptors, which can replace/characterize the recovery curve of the system with the desired level of accuracy. The paper provided a general nomenclature for the resilience metrics and the effect of system properties (including physical characteristics) on

resilience. In addition, the paper discussed the various phases of recovery and their importance in achieving resilience.

For modeling the recovery, the paper proposed a stochastic formulation that models the impact of recovery activities and possible disruptions to recovery by estimating their impact on the damage state of the system. A reliability-based definition of damage levels was developed in this regard, which accounts for the safety requirements and is ideally suited for probabilistic resilience analysis. The proposed model for the recovery process can incorporate information from available databases, collected data, past record and engineering experience, and judgment. A general discussion about the relationship between reliability and functionality is included to better infer and communicate the resilience measured in terms of different types of performance indicators.

Resilience analysis of a RC bridge was performed to illustrate the proposed formulation. Recovery curves and resilience metrics of the bridge were obtained, while considering earthquake hazard and FRP repair strategy. The proposed model is ideally suited in applications such as resilience-based design and life-cycle analysis.

Disclosure statement

No potential conflict of interest was reported by the authors.

Funding

The research presented in this paper was supported in part by the Center for Risk-Based Community Resilience Planning funded by the U.S. National Institute of Standards and Technology (NIST Financial Assistance Award Number: 70NAN-B15H044) and by the Critical Resilient Interdependent Infrastructure Systems and Processes (CRISP) Program of the National Science Foundation (Award Number: 1638346). The views expressed are those of the authors, and may not represent the official position of the sponsors.

Notes on contributors

Neetesh Sharma is a PhD Candidate in the Department of Civil and Environmental Engineering at the University of Illinois at Urbana-Champaign. He has a professional background in civil construction with experience in the energy sector. His research interests include statistical modeling of risk, reliability and resilience of critical infrastructure systems.

Armin Tabandeh is a PhD Candidate in the Department of Civil and Environmental Engineering at the University of Illinois at Urbana-Champaign. His current research centers on risk, reliability and resilience analysis of infrastructure systems.

Paolo Gardoni is a professor and excellence faculty scholar in the Department of Civil and Environmental Engineering at the University of Illinois at Urbana-Champaign, USA. He is the director of the MAE Center which focuses on the creating

of a Multi-hazard Approach to Engineering, and the associate director of the NIST-funded Center of Excellence for Riskbased Community Resilience Planning. He is the founder and Editor-in-Chief of the international journal Sustainable and Resilient Infrastructure. He is internationally recognized for his work on sustainable and resilient infrastructure; reliability, risk and life cycle analysis; decision-making under uncertainty; earthquake engineering; performance assessment of deteriorating systems; ethical, social and legal dimensions of risk; policies for natural hazard mitigation and disaster recovery; and engineering ethics.

References

ATC. (2000). Database on the performance of structures near strong-motion recordings: 1994 Northridge earthquake. Redwood City, CA: Applied Technology Council.

Ayyub, B. M. (2014). Systems resilience for multihazard environments: Definition, metrics, and valuation for decision making. Risk Analysis, 34, 340-355.

Bai, J.-W., Hueste, M. B. D., & Gardoni, P. (2009). Probabilistic assessment of structural damage due to earthquakes for buildings in mid-America. Journal of Structural Engineering, 135, 1155-1163.

Bishop, C. M. (2006). Pattern recognition and machine learning. New York, NY: Springer.

Bocchini, P., Decò, A., & Frangopol, D. M. (2012). Probabilistic functionality recovery model for resilience analysis. In F. Biodini & D. M. Frangopol (Eds.), Bridge maintenance, safety, management, resilience and sustainability (pp. 1920-1927). UK: CRC Press, Taylor and Francis.

Bonstrom, H., & Corotis, R. B. (2016). First-order reliability approach to quantify and improve building portfolio resilience. Journal of Structural Engineering, 142(8), C4014001.

Box, G. E. P., & Tiao, G. C. (1992). Bayesian inference in statistical analysis. New York, NY: Wiley.

Briaud, J.-L., Gardoni, P., & Yao, C. (2014). Statistical, risk, and reliability analyses of bridge scour. Journal of Geotechnical and Geoenvironmental Engineering, 140(2), 4013011.

Bruneau, M., Chang, S. E., Eguchi, R. T., Lee, G. C., O'Rourke, T. D., Reinhorn, A. M., ... von Winterfeldt, D. (2003). A framework to quantitatively assess and enhance the seismic resilience of communities. Earthquake Spectra, 19, 733-752.

Bruneau, M., & Reinhorn, A. (2007). Exploring the concept of seismic resilience for acute care facilities. Earthquake Spectra, 23, 41-62.

Chang, S. E., & Shinozuka, M. (2004). Measuring improvements in the disaster resilience of communities. Earthquake Spectra, 20, 739-755.

Cimellaro, G. P., Reinhorn, A. M., & Bruneau, M. (2010a). Framework for analytical quantification of disaster resilience. Engineering Structures, 32, 3639-3649.

Cimellaro, G. P., Reinhorn, A. M., & Bruneau, M. (2010b). Seismic resilience of a hospital system. Structure and Infrastructure Engineering, 6, 127–144.

Corotis, R. (2009). Societal issues in adopting life-cycle concepts within the political system. Structure and Infrastructure Engineering, 5, 59-65.

Decò, A., Bocchini, P., & Frangopol, D. M. (2013). A probabilistic approach for the prediction of seismic



- resilience of bridges. Earthquake Engineering & Structural Dynamics, 42, 1469-1487.
- Ditlevsen, O., & Madsen, H. O. (1996). Structural reliability methods. Mechanical Engineering. New York, NY: Wiley.
- Duncan, W. (1996). A guide to the project management body of knowledge. Management, 1(11), 459.
- Ellingwood, B. R., Cutler, H., Gardoni, P., Peacock, W. G., van de Lindt, J. W., & Wang, N. (2016). The centerville virtual community: A fully integrated decision model of interacting physical and social infrastructure systems. Sustainable and Resilient Infrastructure, 1, 95-107.
- Gardoni, P. (Ed.) (2017). Risk and reliability analysis: Theory and applications. (P. Gardoni, Ed.). Cham: Springer International Publishing.
- Gardoni, P., Der Kiureghian, A., & Mosalam, K. M. (2002). Probabilistic capacity models and fragility estimates for reinforced concrete columns based on experimental observations. Journal of Engineering Mechanics, 128, 1024-
- Gardoni, P., & LaFave, J. M. (Eds.) (2016). Multi-hazard Approaches to Civil Infrastructure Engineering: Mitigating Risks and Promoting Resilence. Cham: Springer International.
- Gardoni, P., Mosalam, K. M., & Der Kiureghian, A. (2003). Probabilistic seismic demand models and fragility estimates for RC bridges. Journal of Earthquake Engineering, 7, 79-106.
- Gardoni, P., & Murphy, C. (2014). A scale of risk. Risk Analysis, 34, 1208-1227.
- Gardoni, P., Murphy, C., & Rowell, A. (Eds.) (2016). Risk analysis of natural hazards: interdisciplinary challenges and integrated solutions. Cham: Springer International Publishing.
- Gardoni, P., Reinschmidt, K. F., & Kumar, R. (2007). A probabilistic framework for Bayesian adaptive forecasting of project progress. Computer-Aided Civil and Infrastructure Engineering, 22, 182-196.
- Guidotti, R., Chmielewski, H., Unnikrishnan, V., Gardoni, P., McAllister, T., & van de Lindt, J. (2016). Modeling the resilience of critical infrastructure: The role of network dependencies. Sustainable and Resilient Infrastructure, 1, 153-168.
- Guidotti, R., Gardoni, P., & Chen, Y. (2017). Network reliability analysis with link and nodal weights and auxiliary nodes. Structural Safety, 65, 12-26.
- Huang, Q., Gardoni, P., & Hurlebaus, S. (2010). Probabilistic seismic demand models and fragility estimates for reinforced concrete highway bridges with one single-column bent. Journal of Engineering Mechanics, 136, 1340-1353.
- Iervolino, I., Giorgio, M., & Polidoro, B. (2015). Reliability of structures to earthquake clusters. Bulletin of Earthquake Engineering, 13, 983-1002.
- Jia, G., & Gardoni, P. (2017a). A general stochastic framework for modeling deteriorating engineering systems considering multiple deterioration processes and their interactions. Structural Safety, (to be submitted).
- Jia, G., & Gardoni, P. (2017b). Life-cycle analysis of reinforced concrete bridges using a new model for deterioration. Engineering Structures, (to be submitted).
- Jia, G., Tabandeh, A., and Gardoni, P. (2017). Life-cycle analysis of engineering systems: modeling deterioration, instantaneous reliability, and resilience. In P. Gardoni (Ed.), Risk and reliability analysis: Theory and applications (pp. 465-494). Cham: Springer International Publishing.

- Klinger, M., & Susong, M. (2006). The construction project: phases, people, terms, paperwork, processes. Chicago, IL: American Bar Association.
- Kramer, S. L. (1996). Geotechnical Earthquake Engineering. Upper Saddle River, NJ: Prentice-Hall,.
- Kumar, R., & Gardoni, P. (2012). Modeling structural degradation of rc bridge columns subjected to earthquakes and their fragility estimates. Journal of Structural Engineering, 138, 42-51.
- Kumar, R., & Gardoni, P. (2014a). Renewal theory-based life-cycle analysis of deteriorating engineering systems. Structural Safety, 50, 94-102.
- Kumar, R., & Gardoni, P. (2014b). Effect of seismic degradation on the fragility of reinforced concrete bridges. Elsevier Ltd, 79, 267–275.
- Lin, J. (1991). Divergence measures based on the shannon entropy. *IEEE Transactions on Information Theory*, *37*, 145–151.
- McAllister, T. (2013). Developing guidelines and standards for disaster resilience of the built environment: A research needs assessment. Gaithersburg, MD: US Department of Commerce, National Institute of Standards and Technology.
- Means, R. (2008). Building construction cost data. Kingston, MA: Reed Construction Data.
- Mieler, M., Stojadinovic, B., Budnitz, R., Comerio, M., & Mahin, S. (2015). A framework for linking communityresilience goals to specific performance targets for the built environment. Earthquake Spectra, 31, 1267-1283.
- Moselhi, O., Gong, D., & El-Rayes, K. (1997). Estimating weather impact on the duration of construction activities. Canadian Journal of Civil Engineering, 24, 359-366.
- Murphy, C., Gardoni, P., & Harris, C. E. (2011). Classification and moral evaluation of uncertainties in engineering modeling. Science and Engineering Ethics, 17, 553-570.
- Reed, D. A., Kapur, K. C., & Christie, R. D. (2009). Methodology for assessing the resilience of networked infrastructure. IEEE Systems Journal, 3, 174-180.
- Saini, A., & Saiidi, M. S. (2013). Post earthquake damage repair of various reinforced concrete bridge components. Caltrans, Sacramento, CA.
- Sukumaran, P., Bayraktar, M. E., Hong, T., & Hastak, M. (2006). Model for analysis of factors affecting construction schedule in highway work zones. Journal of Transportation Engineering, 132, 508-517.
- Tabandeh, A., & Gardoni, P. (2014). Probabilistic capacity models and fragility estimates for RC columns retrofitted with FRP composites. Engineering Structures, 74, 13-22.
- Tabandeh, A., & Gardoni, P. (2015). Empirical bayes approach for developing hierarchical probabilistic predictive models and its application to the seismic reliability analysis of FRP-Retrofitted RC Bridges. ASCE-ASME Journal of Risk and Uncertainty in Engineering Systems, Part A: Civil Engineering, 1(2), 04015002 (21 p.).
- Takahashi, Y., Der Kiureghian, A., & Ang, A. H.-S. (2004). Lifecycle cost analysis based on a renewal model of earthquake occurrences. Earthquake Engineering & Structural Dynamics, 33, 859-880.
- Yeo, G. L., & Cornell, C. A. (2009a). Building life-cycle cost analysis due to mainshock and aftershock occurrences. Structural Safety, 31, 396-408.
- Yeo, G. L., & Cornell, C. A. (2009b). A probabilistic framework for quantification of aftershockground-motion hazard in California. Earthquake Engineering & Structural Dynamics, 38, 45–60.